



*... for a brighter future*

# ***Particulate Emissions Control by Advanced Filtration Systems for GDI Engines***

***(ANL/Corning/Hyundai CRADA)***

***May 15, 2013***

***DOE Annual Merit Review & Peer Evaluation Meeting***

***PI: Kyeong Lee***

***Postdocs: Seung Choi, Heeje Seong, Yuki Kameya, Hoon Lee***

***Argonne National Laboratory***

***DOE Project Managers: Ken Howden & Gurpreet Singh***

***Office of Vehicle Technologies***

***Project ID: ACE024***



U.S. Department  
of Energy

UChicago ►  
Argonne<sub>LLC</sub>

A U.S. Department of Energy laboratory  
managed by UChicago Argonne, LLC

*This presentation does not contain any proprietary or confidential information*

# Overview

## Timeline

- Start: Oct. 2011
  - Contract signed: Sept. 2012
- 10% Finished

## Budget

- Funding received in FY12
  - DOE: \$500K
  - Corning: \$300K (in-kind)
  - Hyundai: \$110K (in-kind) & \$90K (fund-in)

## Barriers

- Increased back pressure and fuel penalty
- Lack of effective regeneration strategies to reduce input energy
- Underdevelopment of filter materials for GDI PM emissions
- Insufficient information about GDI engine PM emissions

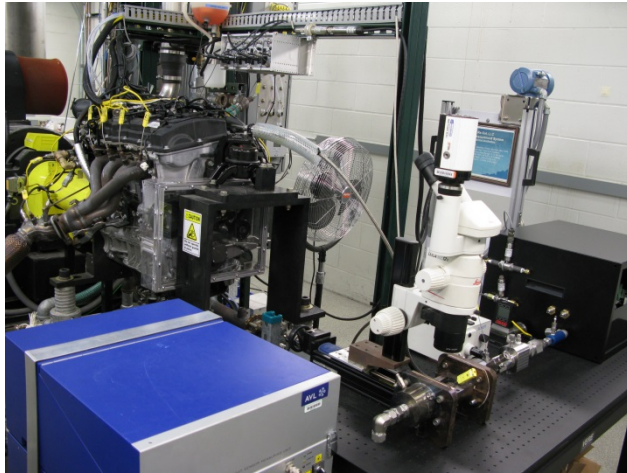
## Partners

- Corning and Hyundai Motor
- University of Wisconsin – Madison
- MIT
- Tokyo Institute of Technology

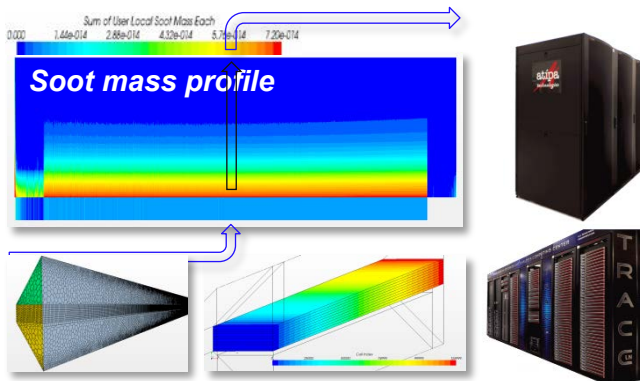
# Relevance and Objectives

- PM emissions are a major problem of GDI engines, but the filtration system (GPF) has not been developed yet.
- GPF system needs to be designed with care, because GDI engines operating at stoichiometric conditions are very sensitive to back pressure.
- Low back-pressure filters are needed to be developed.
- The properties of PM emissions from GDI engines have not been characterized yet.
  
- Evaluate the DPF filtration/regeneration performance as a function of flow condition and porosity.
- Evaluate the level of gaseous emissions and back pressure effects on engine performance to determine the GPF installation position.
- Characterize filtration process for different filter models along with measurement of pressure drop
- Characterize physical properties of PM emissions from a GDI engine.
- Conduct numerical modeling for soot loading in a GPF.

# Approach



GPF experiments for filtration/  
Regeneration with  $\mu$ -imaging



Numerical modeling



2.4L GDI Engine



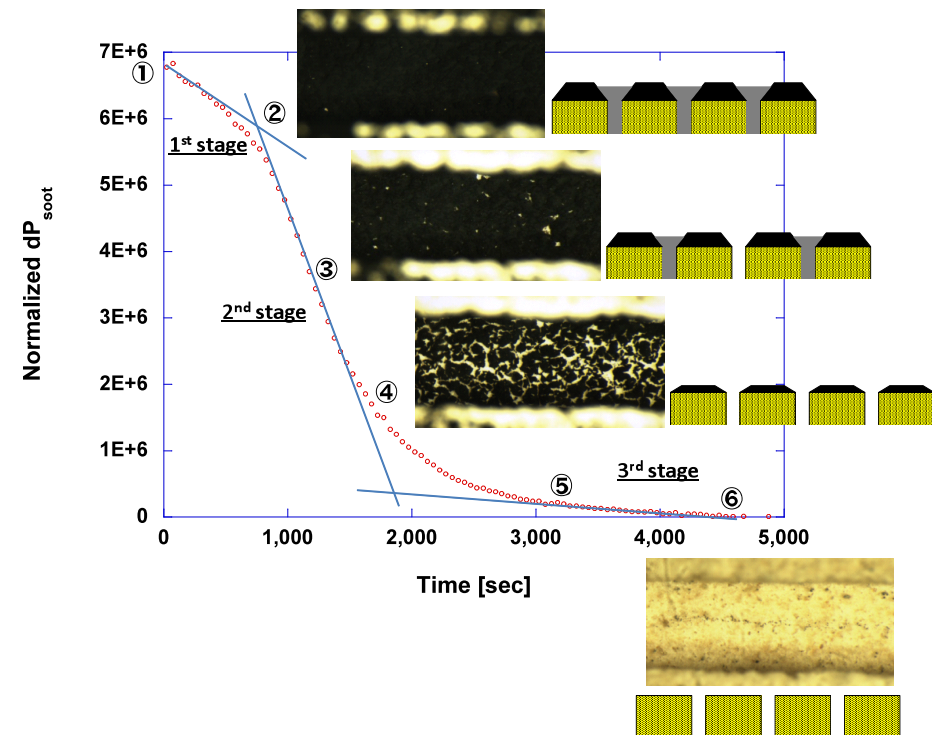
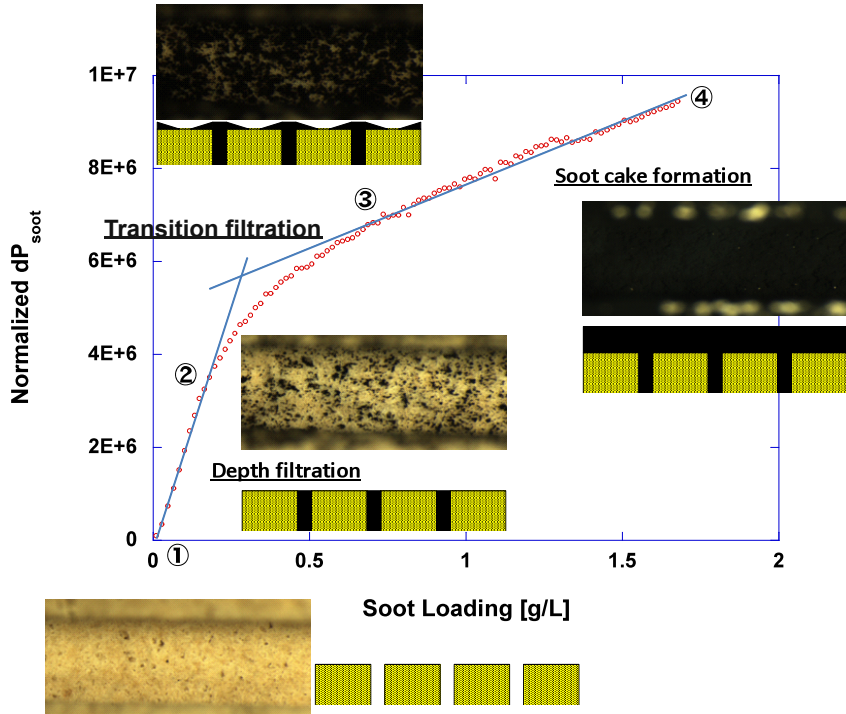
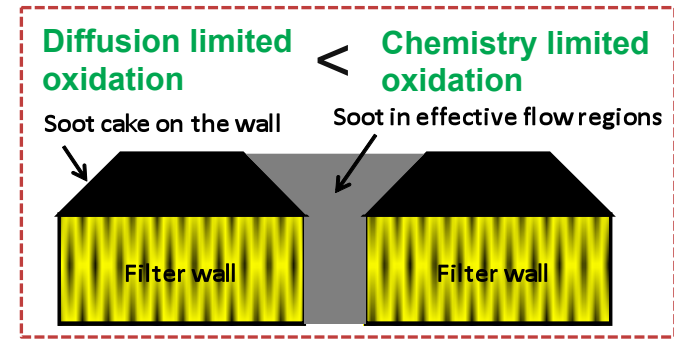
Soot oxidation experiments  
with TGA, DSC, ESEM



X-Ray measurement of soot

# Microscopic visualization further offers understanding of soot filtration and regeneration behaviors in DPFs

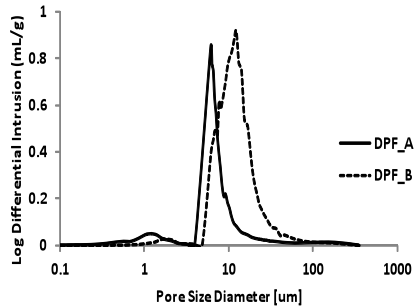
- Pressure drop becomes most significant in the 2<sup>nd</sup> regeneration stage: soot oxidation enhanced in effective flow regions, where surface pores open.
- Soot deposited in pores and effective flow regions oxidizes faster than soot cake on the walls.



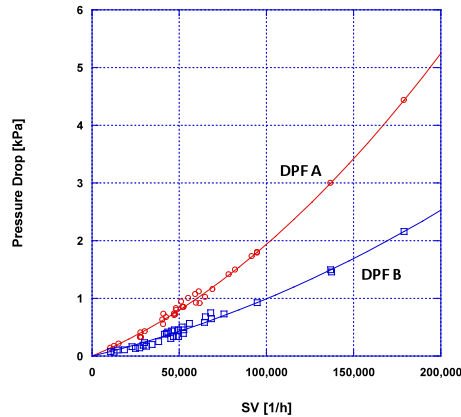
# Experiments were conducted to find the effects of filter structure and emissions flow conditions on pressure drop in filtration

## Filter structure (porosity)

Pore size distribution



Clean filter  $\Delta P$



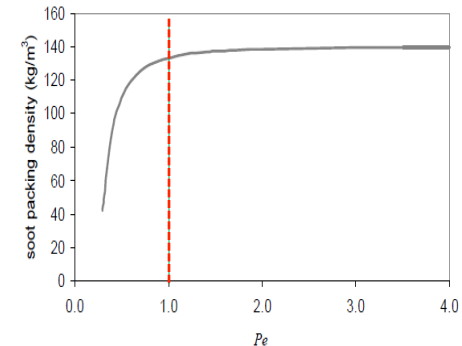
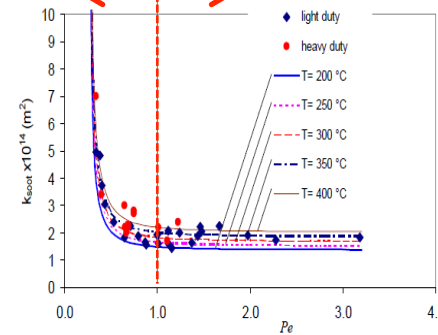
## Flow conditions ( $Pe \#$ )

Low flow: 1500rpm - 4bar  
High flow: 2500rpm - 6bar  
for 2L diesel

$$Pe = \frac{u_w \cdot d_{primary}}{D_p}$$

Convection  
Diffusion

Diffusion dominated ← → Convection dominated

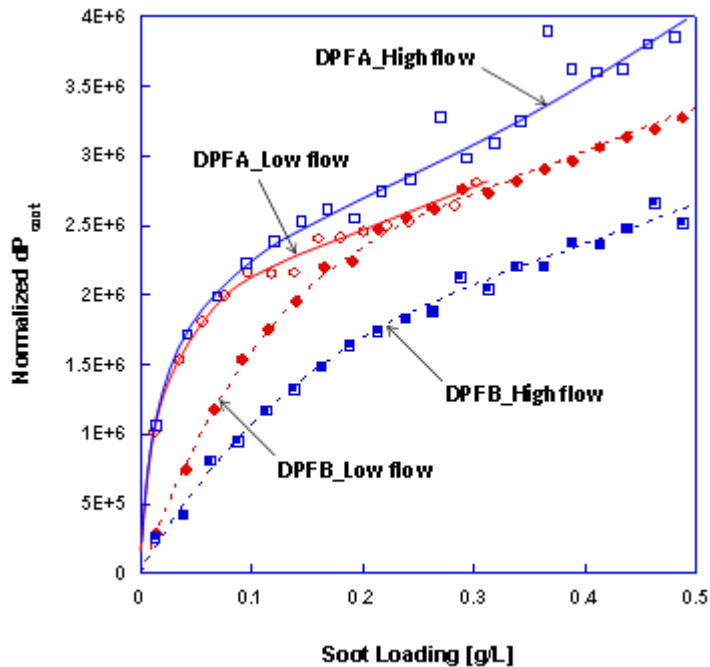


$Pe$  asymptote (Konstandopoulos, SAE 2002-01-1015)

Description	DPF A	DPF B
Size	1.7" square x 6"	1.7" square x 6"
Cell density [cpsi]	200	200
Wall thickness [in]	0.012	0.012
Porosity (effective) [%]	<b>20.89</b>	<b>47.05</b>
Mean pore size ( $d_{50}$ ) [ $\mu\text{m}$ ]	7.242	11.948
Pore size distribution (( $d_{50}-d_{10}$ )/ $d_{50}$ )	0.79	0.41
$d_{10}$ [ $\mu\text{m}$ ]	1.51	7.03
$d_{90}$ [ $\mu\text{m}$ ]	21.13	25.11

	$U_{wall}$ (cm/s)	$Pe_{wall}$	$U_{pore}$ (cm/s)	$Pe_{pore}$
DPF A_Lowflow	0.777	<b>0.236</b>	3.719	<b>1.131</b>
DPF A_Highflow	2.212	<b>0.672</b>	10.587	<b>3.219</b>
DPF B_Lowflow	0.892	<b>0.271</b>	1.894	<b>0.576</b>
DPF B_Highflow	2.233	<b>0.679</b>	4.745	<b>1.442</b>

# Pressure drop by soot depends on flow conditions ( $Pe$ ) and the results propose optimal filter design



## Pressure drop ( $\Delta P_{soot}$ ) during depth filtration

- High porosity filter < Low porosity filter
- No significant difference between convection-dom flows (DPF A).
- Convection-dom flow ( $Pe_{pore} > 1$ ) < Diffusion-dom flow ( $Pe_{pore} < 1$ ) (DPF B)

## Pressure drop ( $\Delta P_{soot}$ ) during soot cake formation

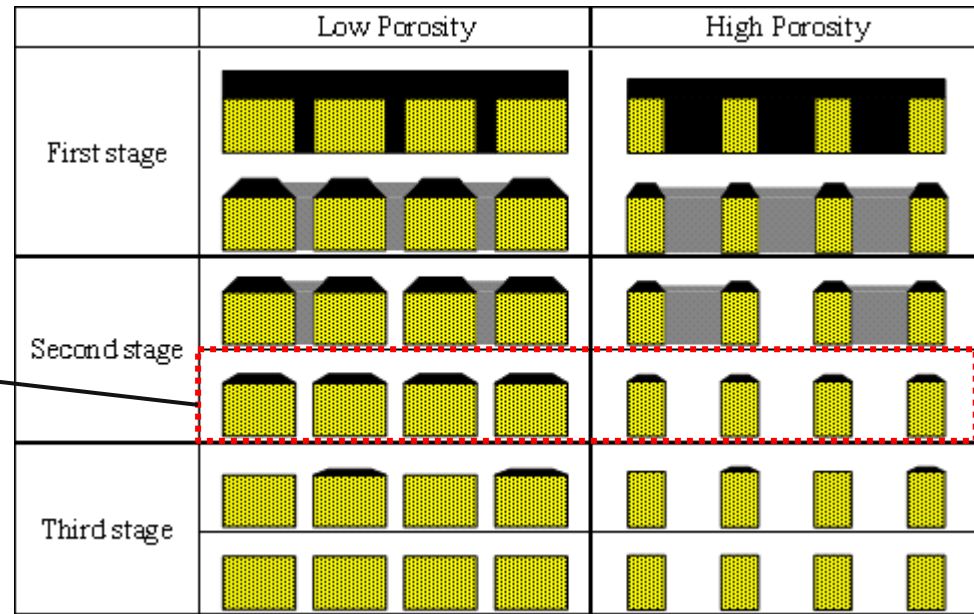
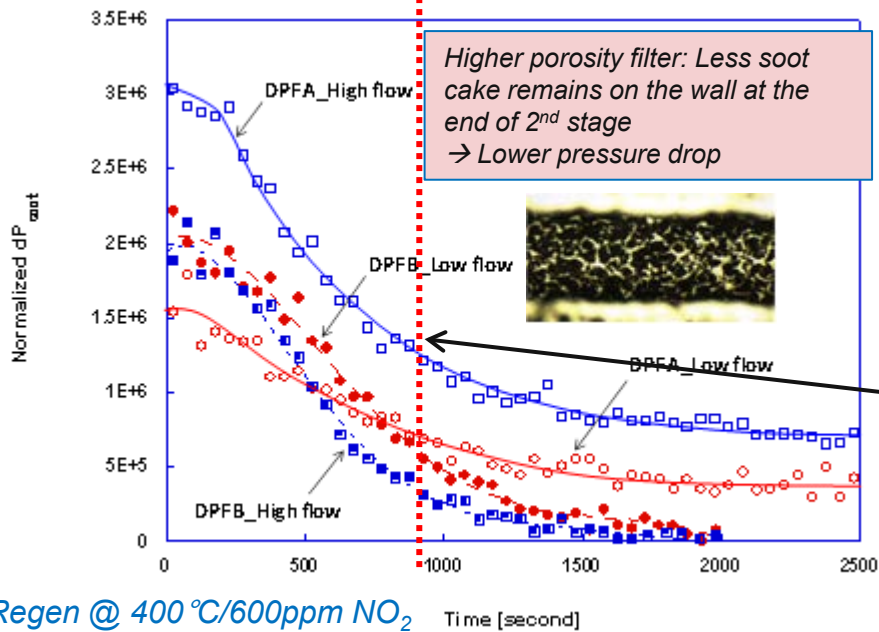
- No consistent correlation between porosity and  $\Delta P_{soot}$
- $\Delta P_{soot}$  correlation found with  $Pe_{pore}$ , but not  $Pe_{wall}$ : because local flows in the 'effective flow region' indeed affect the pressure drop.
- An optimal  $Pe_{pore}$  is about unity (1).

## Optimal flow condition to minimize pressure drop in the entire filtration period

- $Pe_{pore}$  greater than unity (for depth filtration), but as close to unity as possible (for soot cake filtration).
- Filter geometry needs to be designed to meet the optimal  $Pe_{pore}$  condition.

	DPF A Lowflow	DPF A Highflow	DPF B Lowflow	DPF B Highflow
$Pe_{wall}$	0.236	0.672	0.271	0.679
$Pe_{pore}$	1.131	3.219	0.576	1.442
Total soot loading [g/L]	0.313	0.631	0.540	0.598
Soot loading during depth filtration [g/L]	0.034	0.033	0.118	0.163
Gradient of $\Delta P$ profile in depth filtration [Norm. $\Delta P_{soot}/(g/L)$ ]	43,796,817	42,837,006	18,372,021	10,518,552
Gradient of $\Delta P$ profile in soot cake formation [Norm. $\Delta P_{soot}/(g/L)$ ]	2,755,172	4,772,154	3,079,911	2,595,161

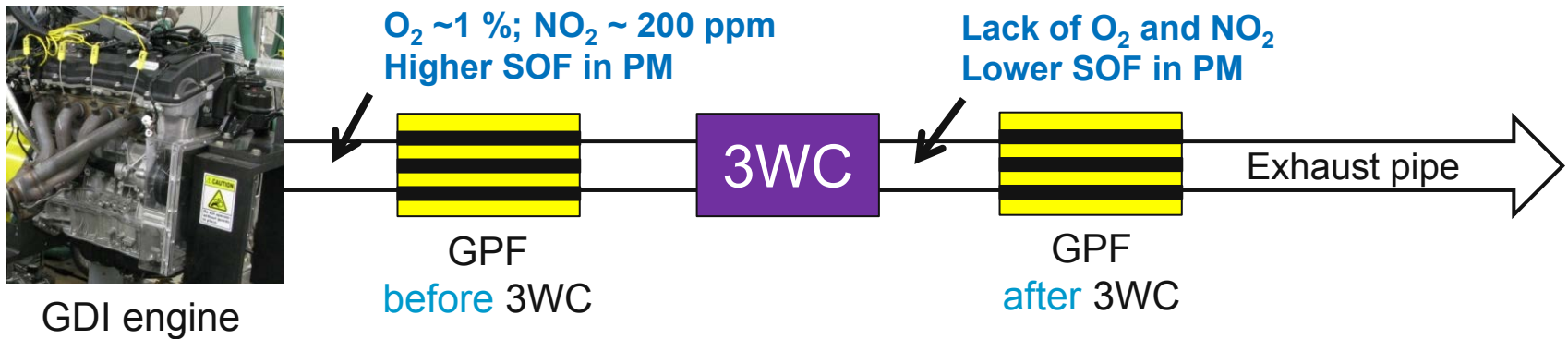
# High porosity filter decreases back-pressure in regeneration and increases regeneration efficiency



- **Regeneration may need to stop at the end of 2<sup>nd</sup> stage**, because the following slow pressure recovery (diffusion-limited) may increase energy consumption.
- **Regeneration time to the end of 2<sup>nd</sup> stage is quite constant**, independent of soot loading conditions ( $Pe$ ) and filter physical properties.
  - **Pressure drop rate =  $f(\text{total soot loading mass})$**
  - **Regeneration efficiency =  $f(\text{filter porosity})$**
- **Higher porosity filter offers better pressure drop recovery and higher regeneration efficiency.**

	DPF A Lowflow	DPF A Highflow	DPF B Lowflow	DPF B Highflow
Total soot loading (g/L)	0.313	0.631	0.540	0.598
Required time to the end of 2 <sup>nd</sup> stage (sec)	1,129	1,013	1,104	864
$\Delta P$ drop rate in 2 <sup>nd</sup> stage (Norm. $\Delta P_{\text{soot}}/\text{sec}$ )	-1,064	-2,141	-2,148	-2,611
$\Delta P_{\text{soot}}$ at end of 2 <sup>nd</sup> stage (Regeneration efficiency)	423,182 <b>(71.8%)</b>	827,054 <b>(71.5%)</b>	294,481 <b>(85.8%)</b>	166,154 <b>(91.5%)</b>

# GPF systems have technical questions to be resolved



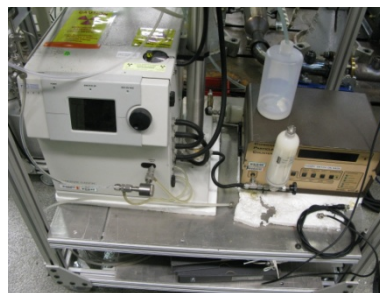
	before 3WC	after 3WC
Pros	<ul style="list-style-type: none"> <li>Existence of <math>O_2</math> and <math>NO_2</math> and <b>high temperature</b> enable continuous regeneration</li> </ul>	<ul style="list-style-type: none"> <li><b>Lower back pressure</b></li> </ul>
Cons	<ul style="list-style-type: none"> <li><b>Longer 3WC heat-up time</b> needed</li> <li><b>Higher back pressure</b></li> </ul>	<ul style="list-style-type: none"> <li><b>Insufficient oxidizers</b> for regeneration</li> </ul>
Questions	<ul style="list-style-type: none"> <li>Proposal of <b>GPF specs</b> suitable for the acceptable pressure-drop limit?</li> <li>Possibility of <b>continuous regeneration</b> and <b>balanced pressure drop</b>?</li> </ul>	<ul style="list-style-type: none"> <li>Regen strategy – engine <b>fuel-cut</b> operation is enough for regeneration, or periodic <b>lean operation</b> is required?</li> <li><b>Effects of soot property changes</b> after 3WC on filtration and regeneration?</li> </ul>

# Hyundai 2.4L GDI engine installation has been completed on a 150 hp AC dynamometer

- Hyundai 2.4L Theta II GDI engine and emissions measurement instruments



Rated power: 148 kW @ 6,300 rpm  
Rated torque: 250 Nm @ 4,250 rpm



<SMPS & CPC>



<Micro Soot Sensor>



<Emission bench>

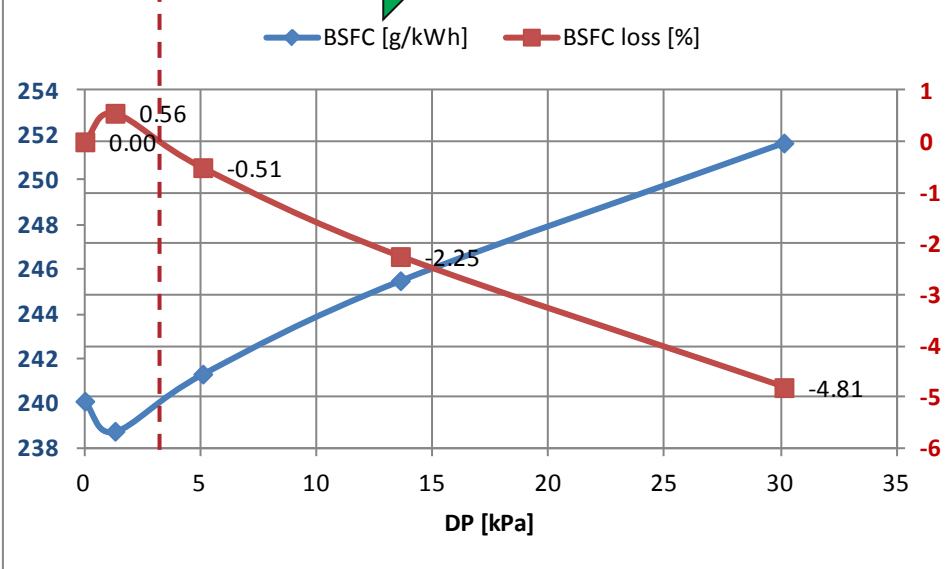
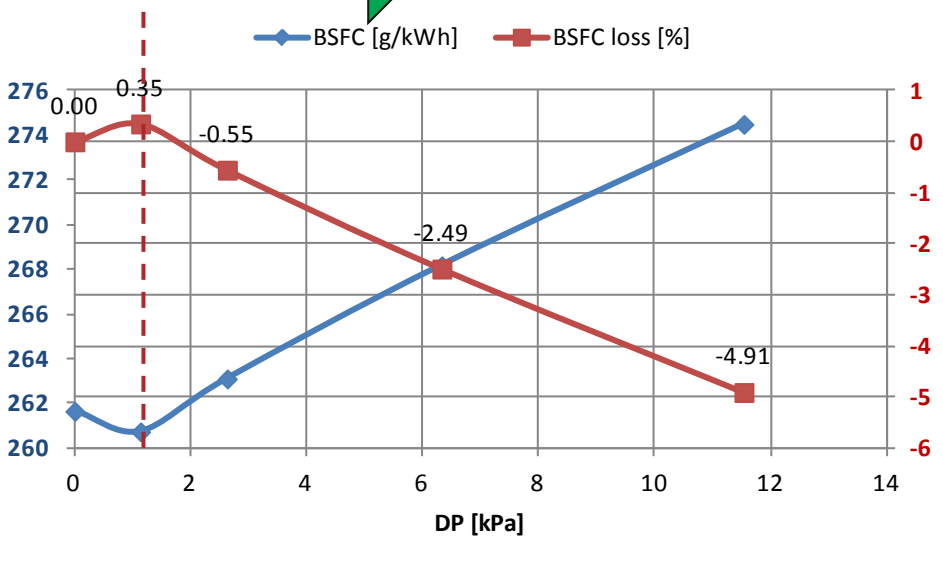
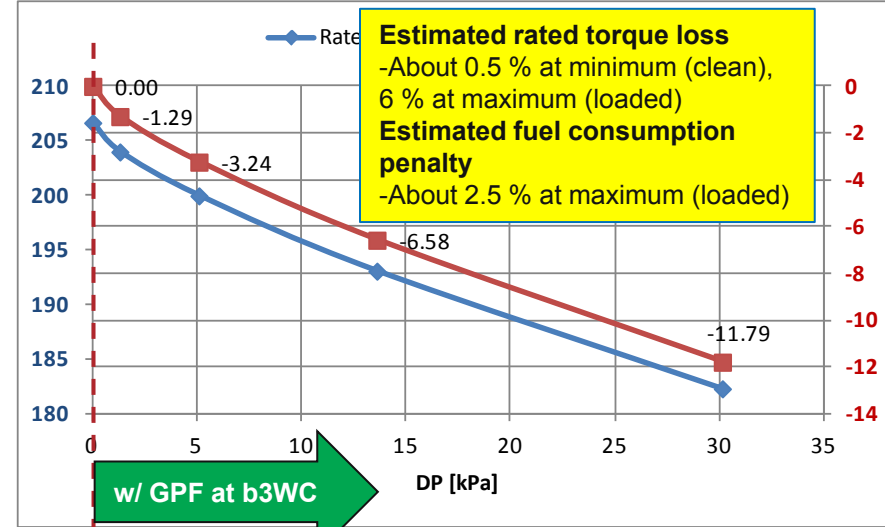
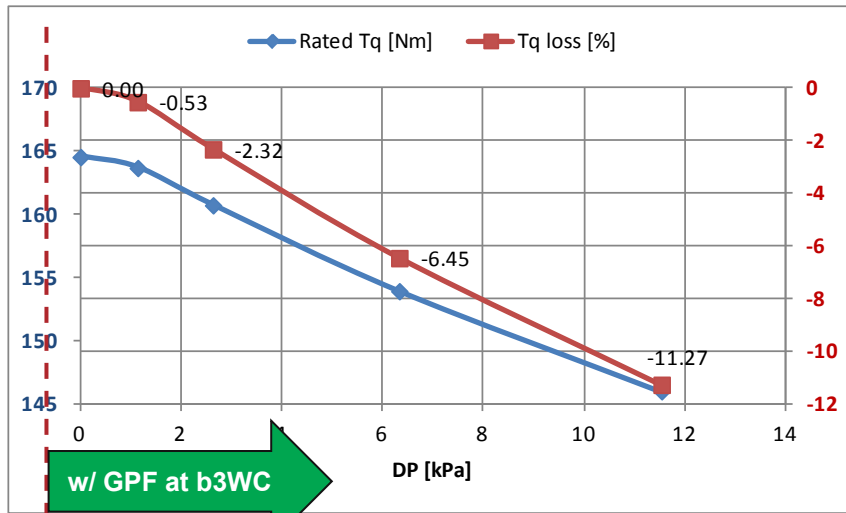


<TEOM>

# Engine performance was evaluated for the case of virtual installation of a GPF b3WC: Torque loss and fuel consumption penalty due to $P_{back}$

<1500 rpm>

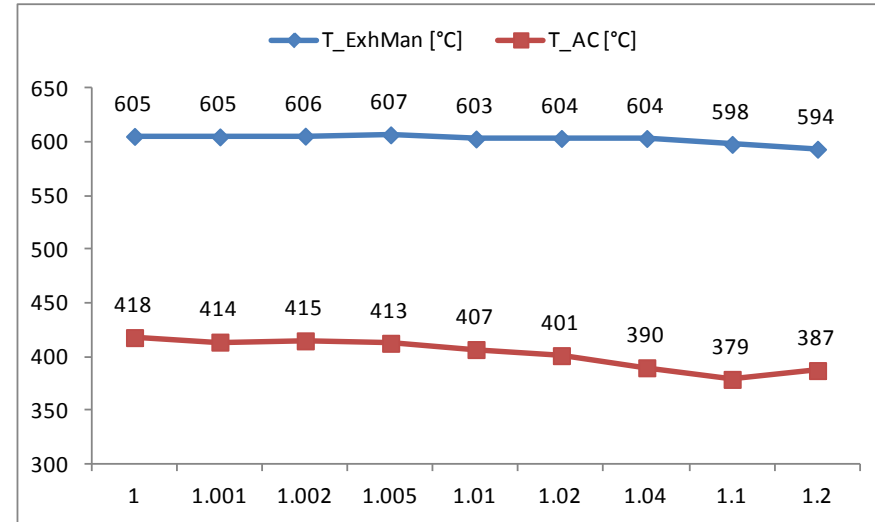
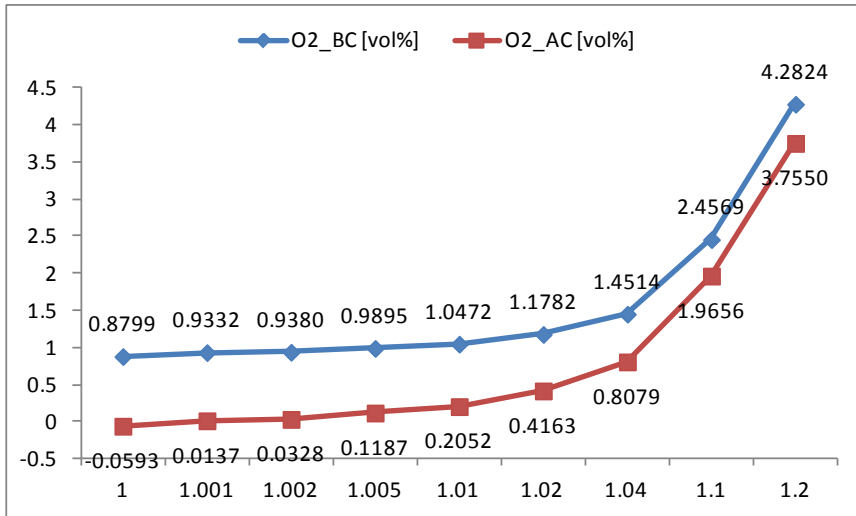
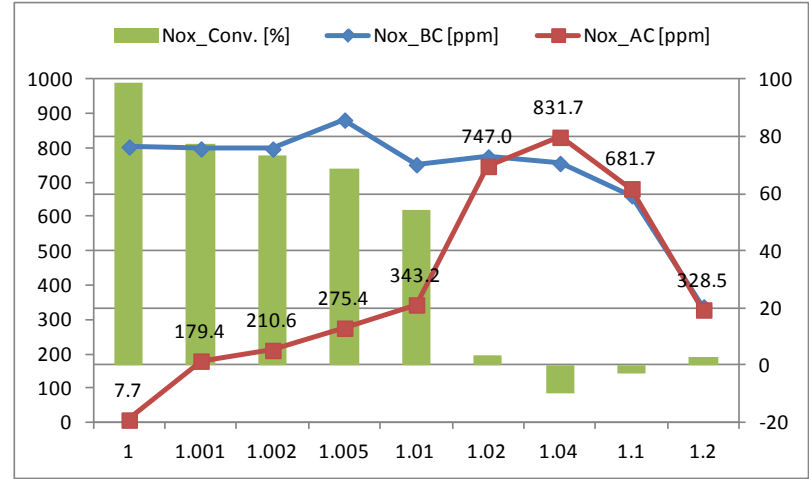
<3000 rpm>



# Changes in oxidizer concentrations at lean-burn conditions were evaluated for GPF regeneration after 3WC

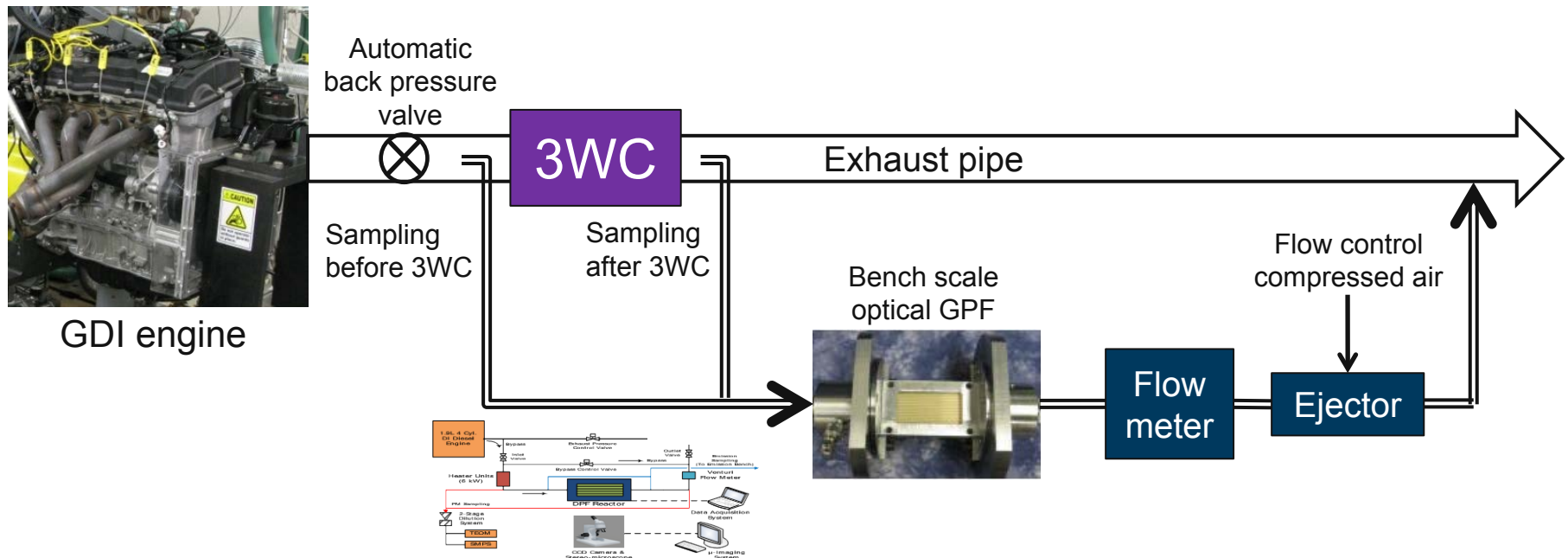
## 1600 rpm / 2.4 bar BMEP

- Lean-burn operation enhanced  $O_2$  concentration, but deteriorated the  $NO_x$  conversion: 0.1%- $O_2$  vs. 70%- $NO_x$  conversion
  - Lean-burn operation may not be applicable to regeneration after 3WC due to the  $NO_x$  penalty.*
- Exhaust temperature cooled down to about 400°C.
- Therefore, fuel-cut effects will be evaluated.

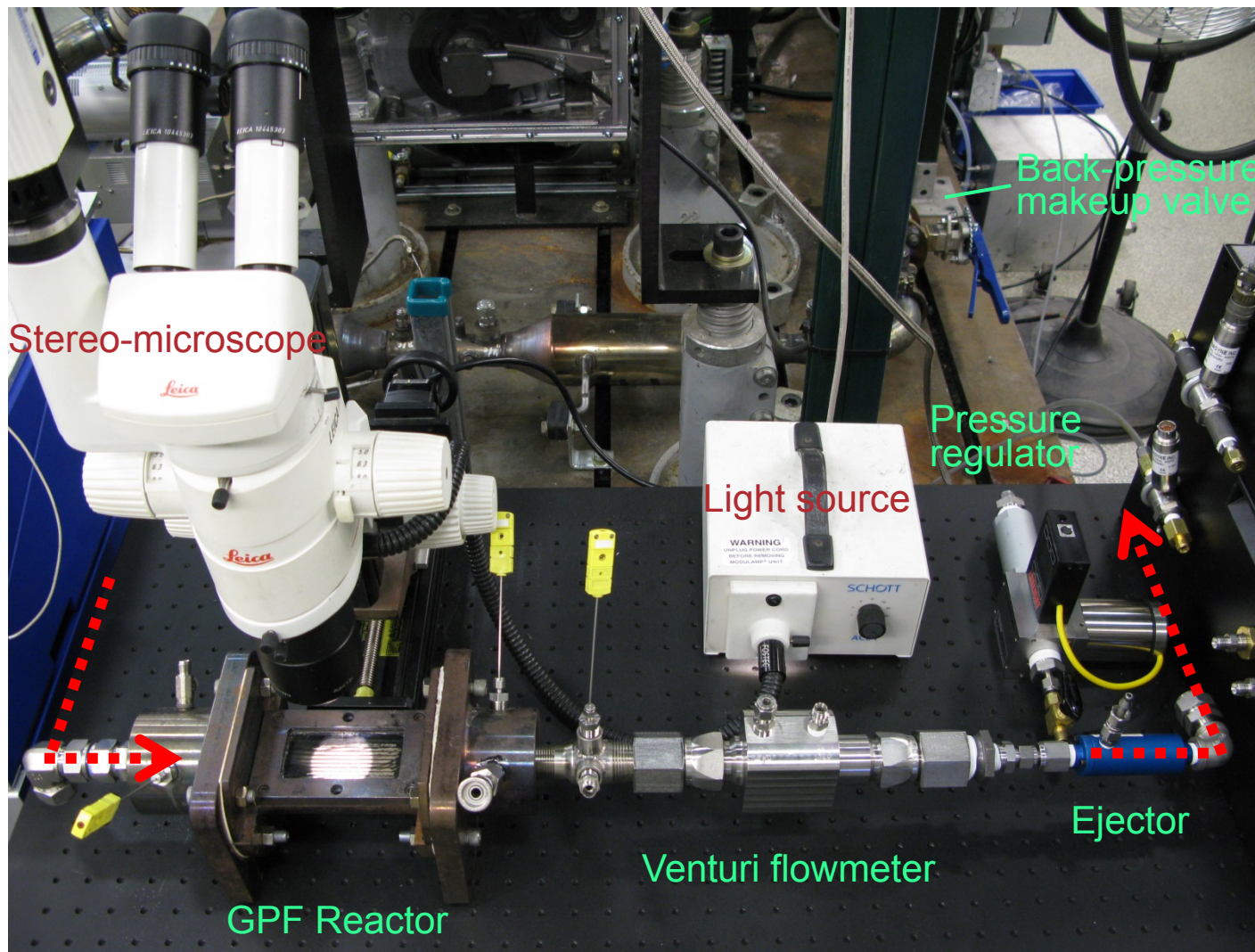


# The test bench was fabricated with automatic engine exhaust back-pressure and sample flowrate control systems

- Bench-scaled (2" x 6" bisected) optical GPF test system
  - Engine back-pressure and emissions flowrate are automatically controlled to simulate practical GPF system.
  - Microscopic processes of soot filtration/regeneration will be visualized in filter channels, along with pressure drop measurements.
  - Filtration/regeneration experiments will be conducted both before and after three-way catalyst (3WC)



# A new GPF bench test system has been fabricated



# *In-situ observation of soot cake oxidation using E-SEM*

## ■ Microscopic observation of DPF regeneration

- Soot cake layer deformation during oxidation
- Soot-catalyst contact (e.g., loose or tight)
- This work enables us to analyze oxidation behaviors of soot cake at a microscopic scale.

## ■ Environmental Scanning Electron Microscope (E-SEM)

- In-situ observation of soot oxidation at micro-scales
- Chamber conditions
  - *Wide range of pressure change (vacuum to 2.6kPa)*
  - *Various reactant gases, such as air, oxygen*
  - *Temperature controllable up to  $T_{max} = 1500\text{ }^{\circ}\text{C}$*
  - *Quasi-steady state in the chamber.*

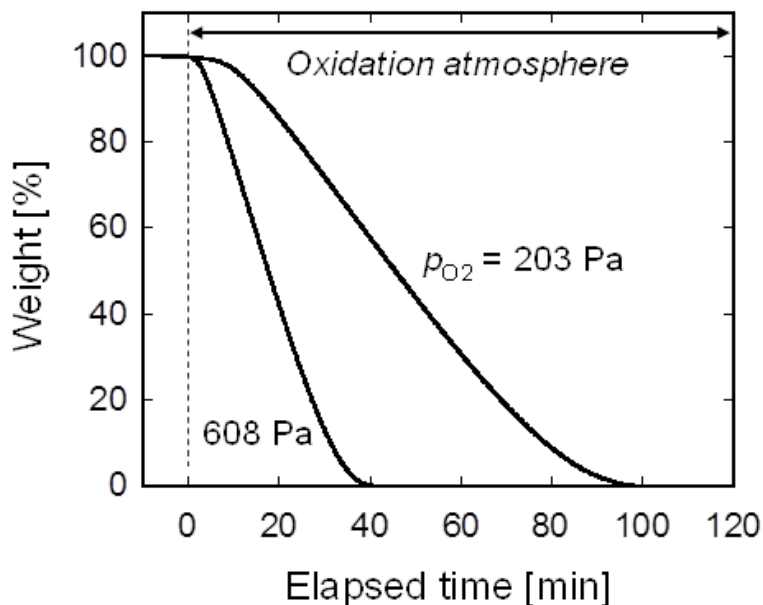


# E-SEM visualizes soot cake oxidation on a filter membrane at a real time

## ■ Thermogravimetric analysis

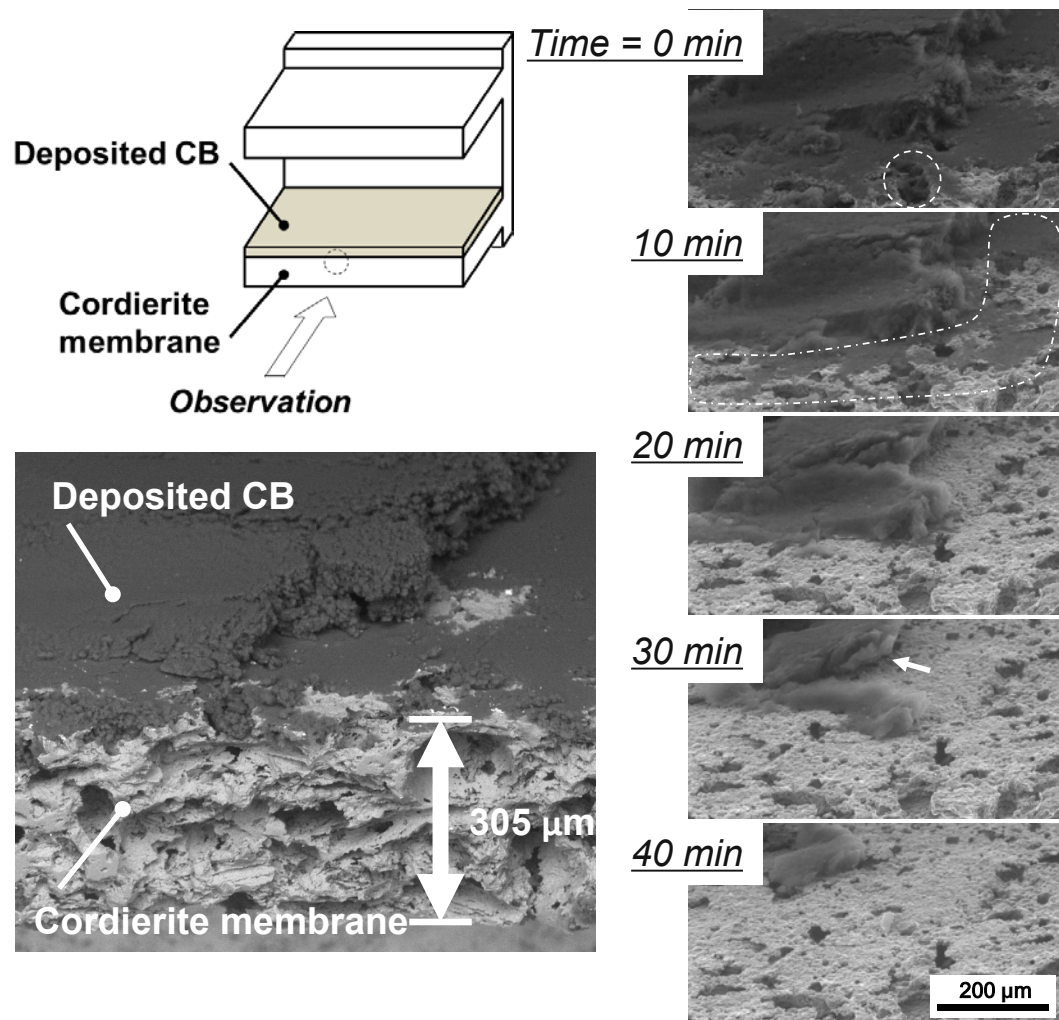
*Isothermal analysis at 800°C*

Surrogate soot (carbon black)



- To complete oxidation within 60 min, 4.0 Torr (533 Pa) of O<sub>2</sub> was used in ESEM experiments

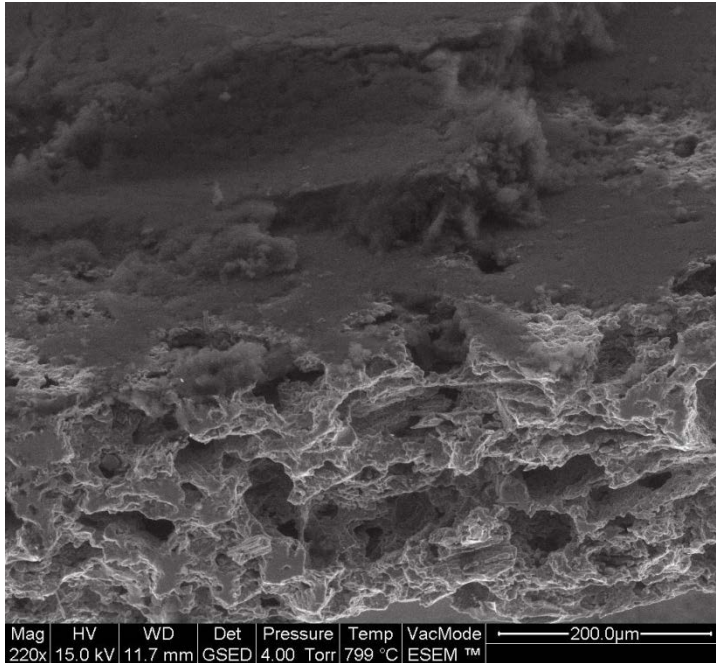
## ■ ESEM observation (800°C, 4.0 Torr O<sub>2</sub>)



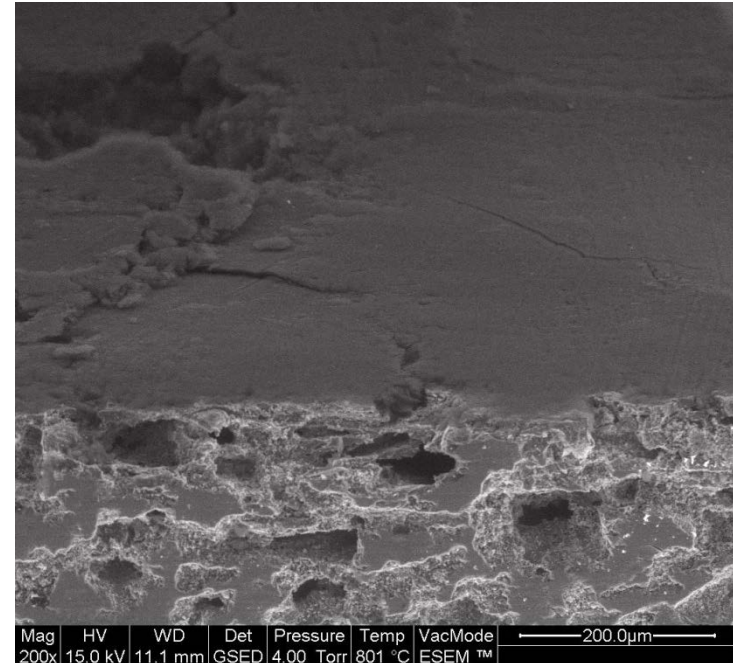
# Catalyst coating on DPF demonstrates significantly different oxidation behaviors

Surrogate soot (carbon black), 800°C, 4.0 Torr of O<sub>2</sub>

**(1) Cordierite w/o catalyst**

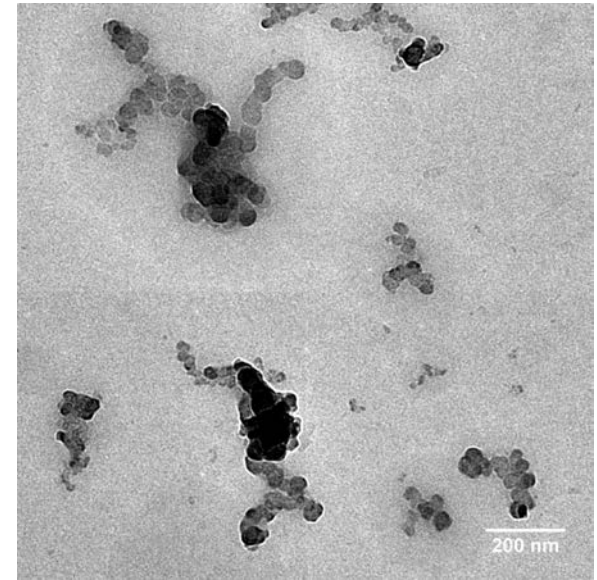
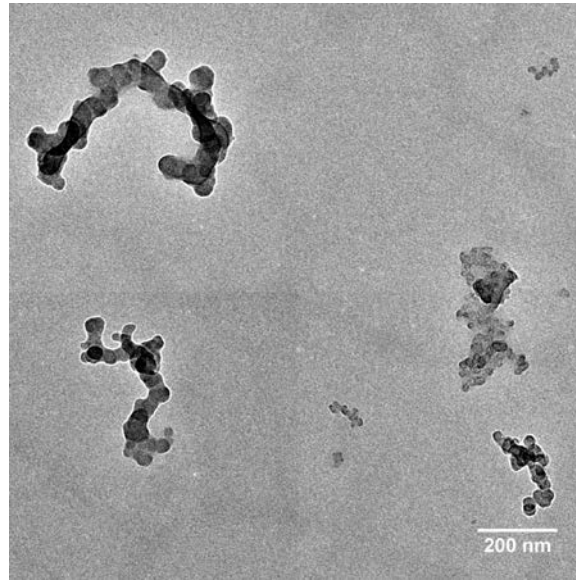
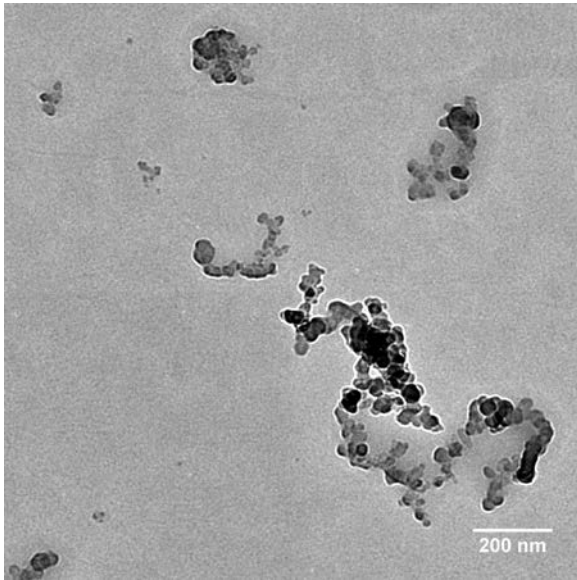


**(2) Pt-catalyst coated**



- (1) Relatively firm contact of soot cake with the substrate: Oxidation shrinks soot cake as a bulk solid material.
- (2) Loose contact of soot cake: The contact condition needs to be enhanced to utilize the catalytic effects.

# TEM revealed a wide range of particulate size from a GDI engine (collaboration with UW-ERC)



Gasoline,  $\phi = 0.98$ ,  $310^\circ$  bTDC

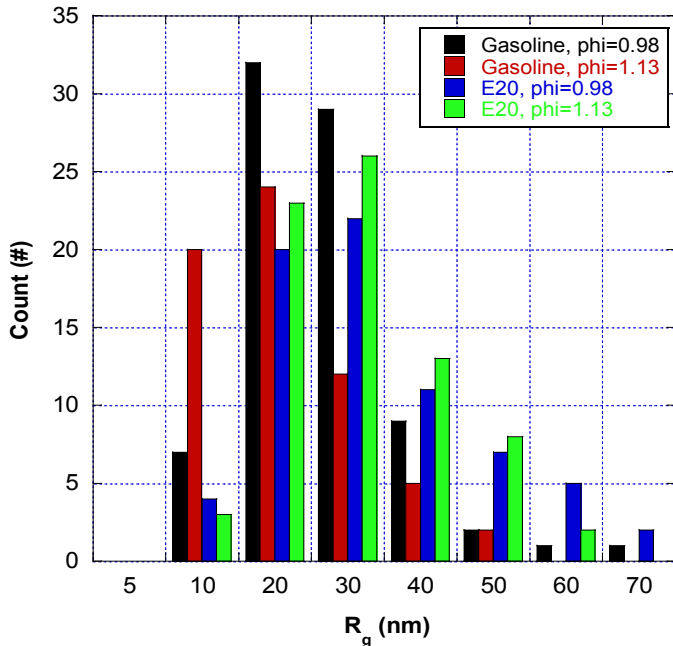
Gasoline,  $\phi = 1.13$ ,  $310^\circ$  bTDC

E20,  $\phi = 0.98$ ,  $310^\circ$  bTDC

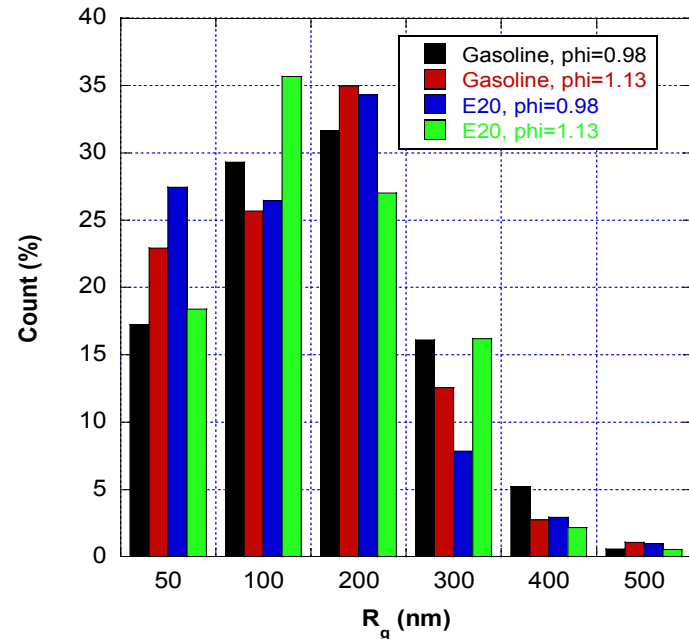
- 549 cc single-cylinder GDI engine; 2100 rpm/650 kPa IMEP; Inj. time: 220 –  $310^\circ$  bTDC
- Two different categories of particles were clearly observed:
  - Aggregates of small primary particles ( $d_p = 5\text{-}10$  nm)
  - Aggregates of large primary particles ( $d_p = 20\text{-}50$  nm).
- Single nanoparticles were found to be smaller than 10 nm in diameter.

# Detailed image analysis revealed two distinct particle size distributions (at 310° bTDC)

## ❖ Aggregates of small primary particles



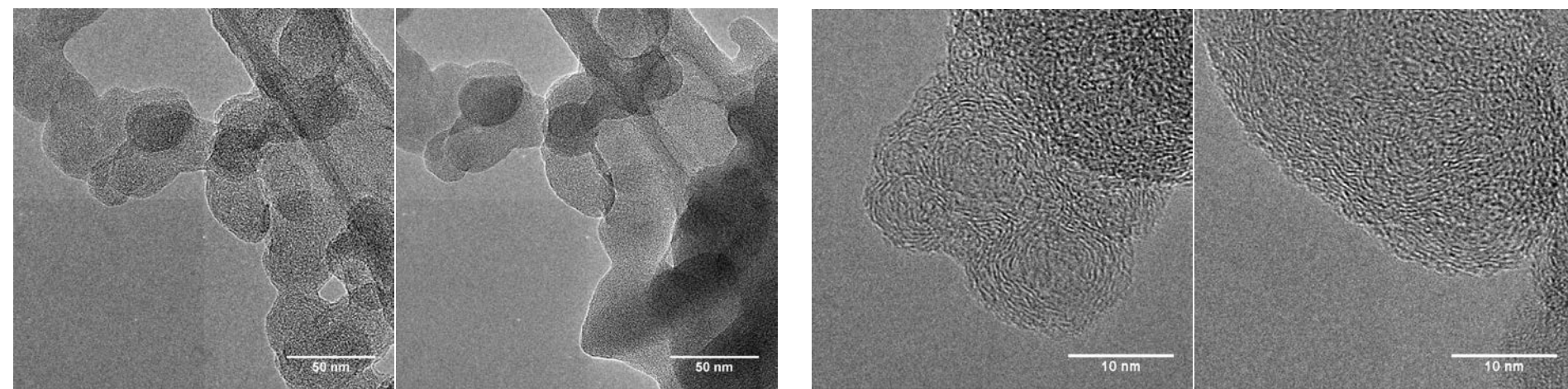
## ❖ Aggregates of larger primary particles



- Aggregates with small primary particles lies in a size range of  $R_g=5$  to 70 nm, while those with large primary particles in a size range of  $R_g=25$  to 500 nm.
- The advancement of fuel injection timing seems to be responsible for generating two different categories of particle sizes (e.g., fuel impingement)
  - Large aggregates with large  $d_p$ : contribution of hydrocarbons to soot growth.
  - Small aggregates with small  $d_p$ : inception of nascent soot particles.

# *GDI particles exhibited complexity in nanostructure*

❖ E20,  $\phi = 1.13$ , 280° bTDC



Initial image

Image after 600kX

Image 1 at 600kX

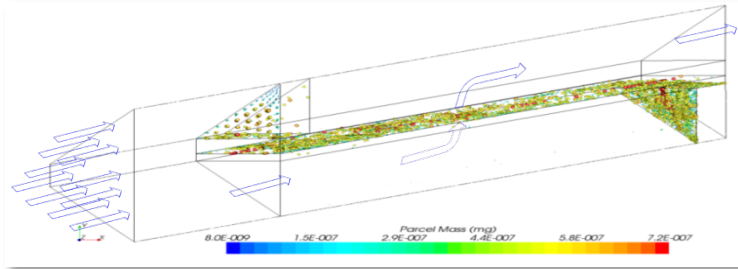
Image 2 at 600kX

- Soot particles from E20 were often observed to expand and change the nanostructure at high magnifications (high electron energy), which has rarely been observed for diesel particles.
- Detailed examination on nanostructure revealed particles present at different levels of soot graphitization.
- Differences in nanostructures appeared to be insignificant with variations of fuel injection timing, fuel type and equivalence ratio.

# Two different approaches were used for soot filtration modeling

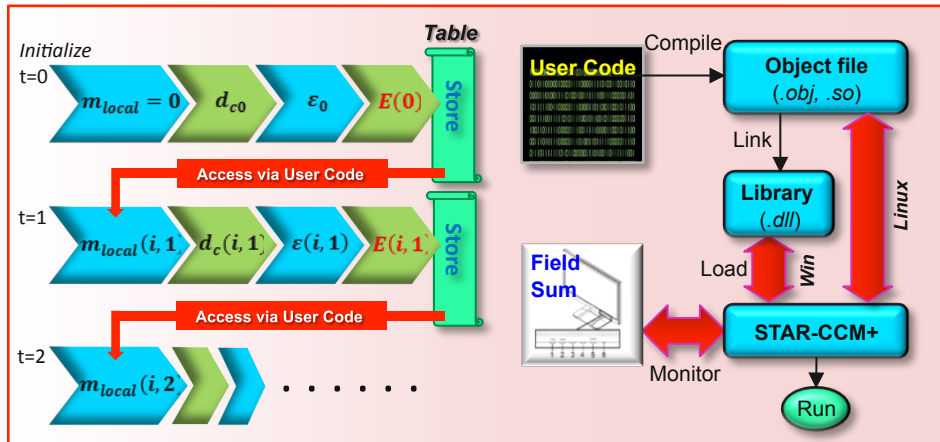
## ■ Lagrangian approach (FY11)

- Objectives: Qualitative analysis by tracking particles trajectories with appropriate B.C.s.

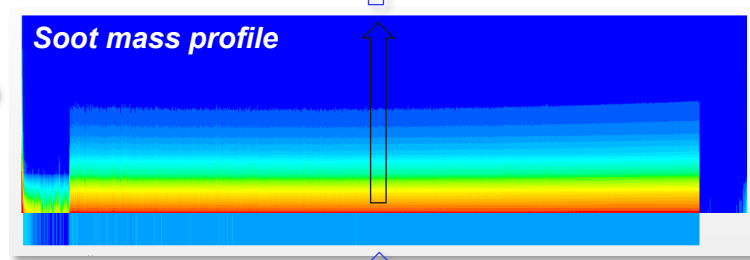
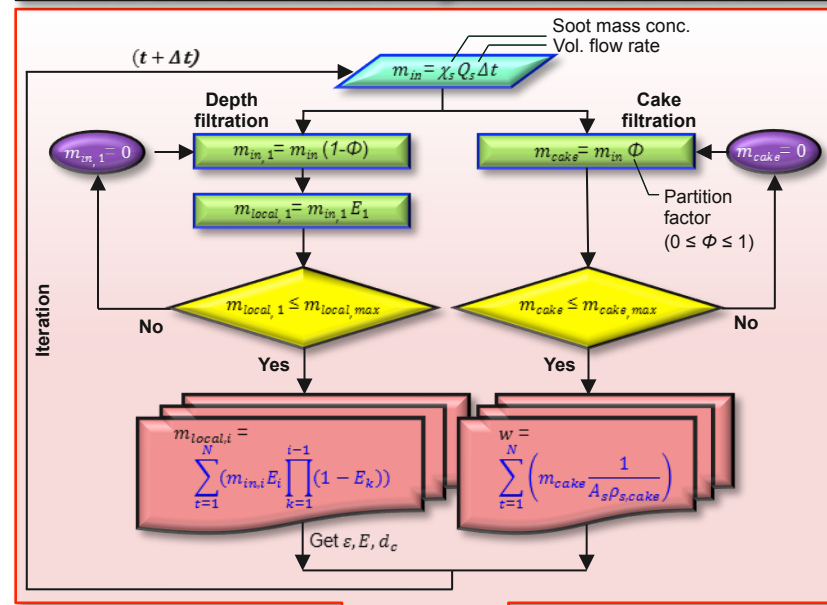


## ■ Eulerian approach (FY12)

- Objectives: Quantitative analysis of local values of filtration parameters by integrating user codes.



## Numerical algorithm applied via self-developed user subroutines is integrated in the CFD code

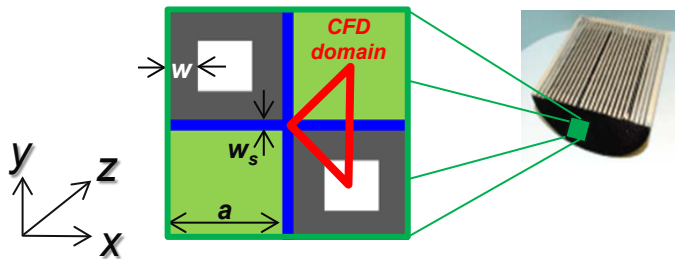


# A 3-D CFD model has been developed for detailed numerical analysis of soot filtration processes

## ■ CFD domain setup

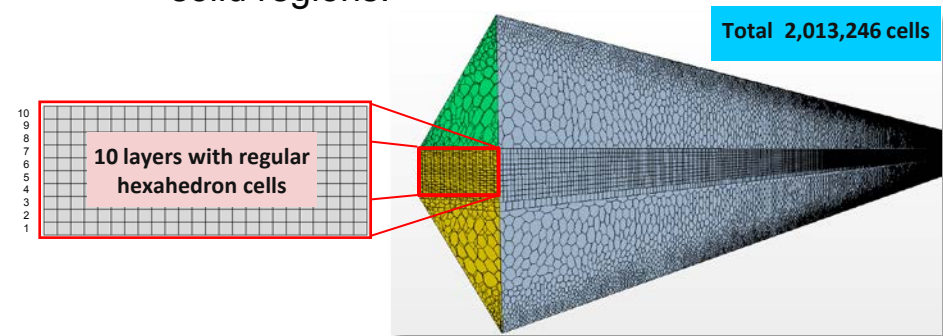
- Geometry: 200 cpsi, lab-scale (2" x 6") cordierite filter with regions of upstream and soot cake.

Upstream=L 0.78", Plug= L 0.39",  $w_s=12.0$  mils



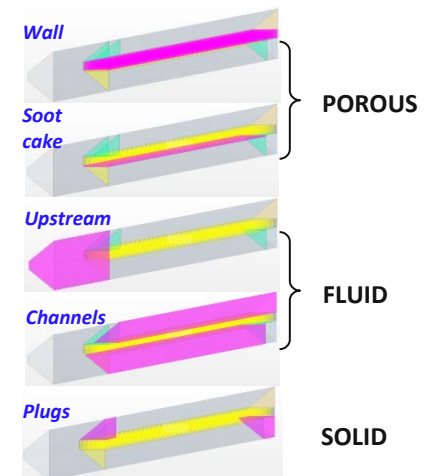
## ■ Meshing

- Volume meshes are generated by **Trimmer** for porous regions and **Polyhedral** for fluid and solid regions.



## ■ Physical assumptions for model setup

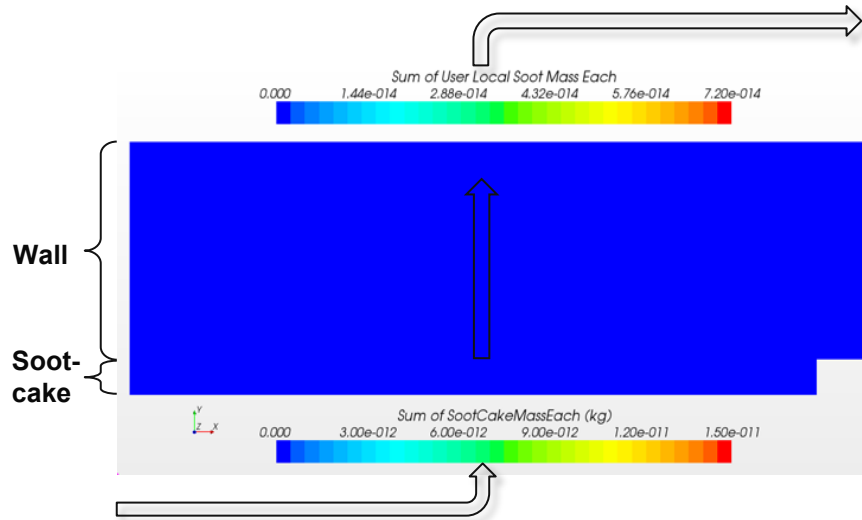
1. Fluid: 3D, Ideal gas, Laminar, Incompressible
2. Implicit unsteady (2<sup>nd</sup> order temporal discretization)
3. Segregated flow solver (2<sup>nd</sup> order convection scheme,  $URF=0.5P, 0.2V$ )
4. Convective heat loss
5. No flow in axial(z) direction in wall regions
6. PM is homogeneously distributed in the flow
7. PM properties ( $d_p=54.5$  [nm],  $\rho_p=2.87$  [g/cm<sup>3</sup>]) are estimated from experiments



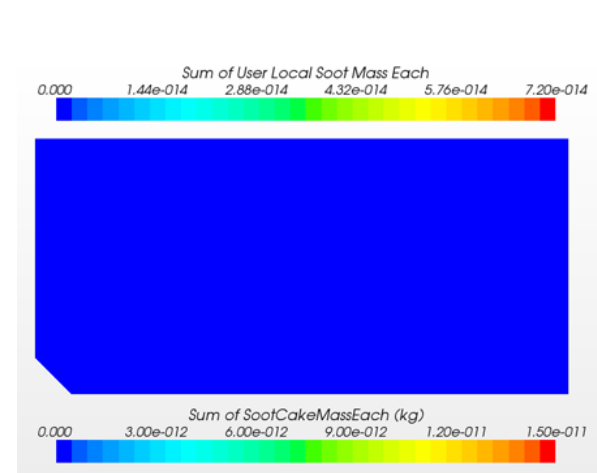
# Modeling Results (Simulation duration: 35 min)

## ■ Temporal evolution of local soot mass

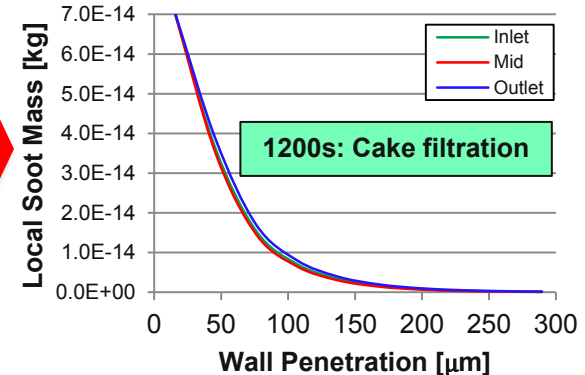
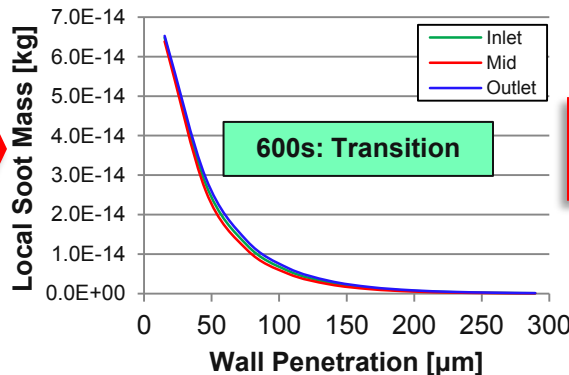
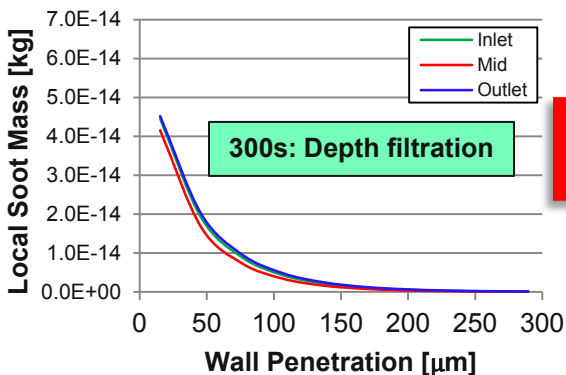
□ y-z plane view (@  $x = 1/4a$ )



□ x-y plane view (@  $z = 1/2L$ )



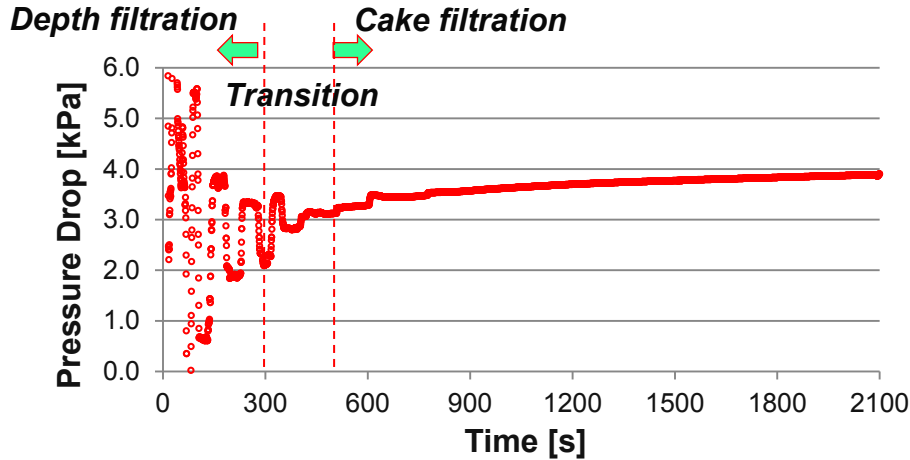
## □ Deposited soot profiles



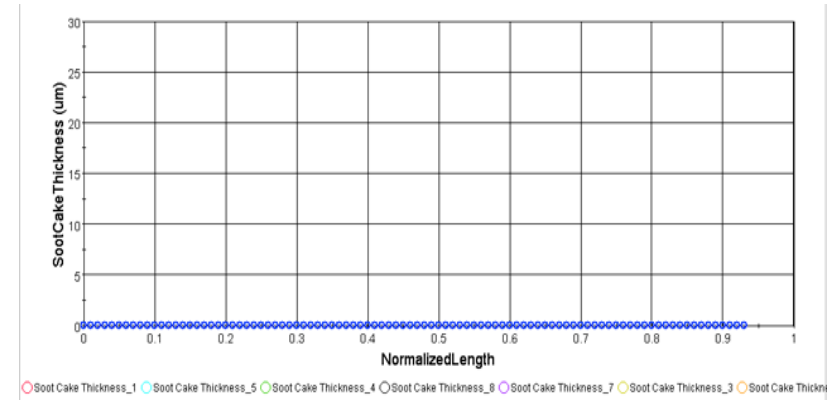
# Modeling Results (Simulation duration: 35 min)

## ■ Temporal evolution of the other filtration parameters

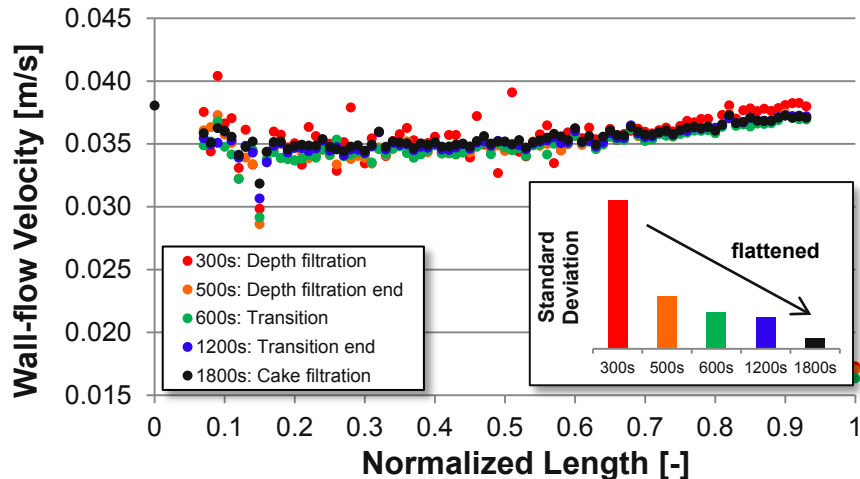
□ Pressure drop - overall



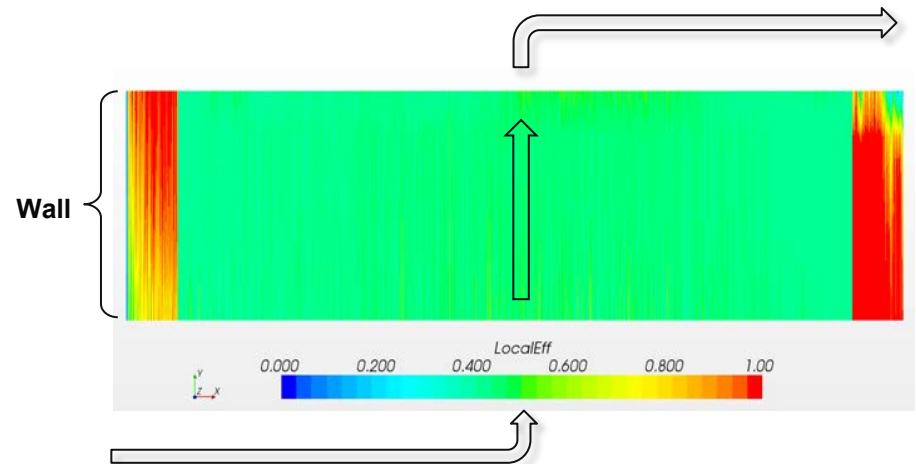
□ Soot cake profile



□ Wall-flow velocity profile



□ Local collection efficiency



# Future Work

- Evaluate the filtration/regeneration performance for various filter models.
- Evaluate filtration/regeneration performance with catalyzed GPF.
- Evaluate kinetics of soot oxidation from the GDI engine with different compositions of reactant gases, using TGA and DSC
- Characterize the physical properties of PM emissions from the GDI engine as a function of engine operating condition, sampling position, and fuel injection timing.
- Characterize soot cake deformation during oxidation at various ambient conditions, using E-SEM.
- Conduct numerical modeling for G(D)PF regeneration at various conditions

# Summary

- Strategies for low pressure drop and high regeneration efficiency were proposed by controlling the flow condition ( $Pe$ ) and filter porosity, respectively.
- GDI engine performance (torque, BSFC) was evaluated for virtual GPF installation before the catalyst.
- Lean-burn conditions slightly increased  $O_2$  concentration after the catalyst, while  $NO_x$  conversion efficiency decreased quite a bit.
  - Lean-burn operation may not be applicable to regeneration after 3WC.
  - Fuel-cut effects will be evaluated.
- E-SEM experiments showed a potential to examine the in-situ oxidation behaviors of soot cake at a high spatial resolution.
- TEM analyses revealed that GDI engine generated numerous nanoparticles and two different size categories of aggregates. In addition, nanostructure analysis for E20-derived soot particles found different levels of graphitization (280° bTDC).
- Numerical modeling was successfully conducted for soot-laden flow in a cordierite filter, in which the self-developed user subroutines were implemented to the CFD code.

# Accomplishment

## ■ Publications

### – Journals (2)

- Chong, H., Aggarwal, S., Lee, K., Yang, S., and Seong, H.: “Experimental Investigation on the Oxidation Characteristics of Diesel Particulates Relevant to DPF Regeneration,” *Journal of Combustion Science and Technology* (2012).
- Lee, K., Seong, H., and Choi S.: “Detailed Analysis of Kinetic Reactions in Soot Oxidation by Simulated Diesel Exhaust Emissions,” 34<sup>th</sup> International Symposium on Combustion (2012).

### – Conference Proceedings and Workshops (4)

- Seong, H, Lee, K., and Choi, S.: “Characterization of Particulate Morphology, Nanostructures, and Sizes in Low-Temperature Combustion with Biofuels,” SAE 2012-01-0441.
- Seong, H. and Lee, K.: “Kinetic Study on Soot Oxidation by Simulated Diesel Gas Emissions,” 2012 CLEERS Workshop, Dearborn, MI, May 2, 2012.
- Choi, S., Lee, K, and Seong H.: “Characterization of Pore Structures in Diesel Particulate Filters by Mercury Intrusion Porosimetry, optical Imaging, and X-Ray Micro-tomography,” AFS 2012 Annual Conference, Boca Raton, FL, June 6, 2012.
- Lee, K., Seong, H., Church, W., and McConnell, S.: “Examination of Particulate Emissions from Alcohol Blended Fuel Combustion in a Gasoline Direct Injection Engine,” 2012 COMODIA, Fukuoka, Japan, July 23-26, 2012.

# Contact

**Kyeong Lee**

Argonne National Laboratory

- (630)252-9403
- *klee@anl.gov*